Observation of resonant Raman scattering at the Si $L_{2,3}$ core exciton

S. Shin, A. Agui, M. Watanabe, M. Fujisawa, Y. Tezuka, and T. Ishii
Synchrotron Radiation Laboratory, Institute for Solid State Physics, University of Tokyo, Tanashi, Tokyo 188, Japan
(Received 15 August 1995; revised manuscript received 16 February 1996)

The resonant soft-x-ray emission spectra at the Si $L_{2,3}$ core exciton have been measured at 18 K by using synchrotron radiation. As an excitation light source, a very high-resolution monochromator with the undulator was used. The Raman scattering whose energy shifts in proportion to the excitation energy is found below the $L_{2,3}$ absorption edge. The intensity of the Raman scattering increases rapidly as the excitation energy comes close to the $L_{2,3}$ core exciton. It is found that the Raman scattering resonates at the $L_{2,3}$ core exciton which is made around the X_1 conduction minimum. The elementary excitation of the Raman scattering is the valence exciton that is a transition from X_1 or X_4 points in the valence band to the X_1 conduction minimum. The X_4 valence exciton has a characteristic excitation-energy dependence, so that it becomes broad and weak as the resonant Raman process goes to the ordinary Raman process. [S0163-1829(96)02824-X]

I. INTRODUCTION

Soft-x-ray emission spectroscopy (SXES) has been one of the most important experimental methods to study the electronic structure of solids. SXES has been carried out for a long time by using a high-power x-ray tube or electron emission source. Very recently, SXES has been carried out by using synchrotron radiation, which is a tunable excitation-light source.[1] These studies provide many insights into the interaction of matter and light. First, the valence states drawn out by the electronic transition to the core level are the partial density of states (DOS) that are projected to the same atomic site where the core hole is produced, since the wave function of a core hole is quite localized. Also, their symmetries are restricted by the selection rule, since its angular momentum symmetry is well defined due to the dipole transition. Synchrotron radiation enables us to excite the specified core level for the specified ion. Thus SXES is a powerful tool to observe the site-projected and symmetry-restricted partial DOS curves. Second, inelastic light scattering has been found in the SXES of diamond,[2,3] graphite,[4] and Si,[5,6] where the electron wave vector (**k**) conservation model has been proposed. That is, the **k** of the produced core hole is the same as that of the excited electron within the small wave vector of the photon. Furthermore, SXES is bulk sensitive, because the mean free path of the soft-x-ray light is much longer than that of the electron. This site- and symmetry-selective nature as well as surface insensitivity is quite distinctive of SXES, and advantageous as compared with the photoelectron spectroscopy (PES).

In this study, resonant soft-x-ray emission (SXE) spectra on Si have been measured in order to clarify the inelastic light-scattering effect. The very high-resolution monochromatized light enables the selective excitation to the conduction bands, and gives us fruitful information on the resonance state of the SXES. That is, what state is the resonance state in SXES? There is also the problem of whether the Raman-scattering effect is found in the soft-x-ray region, and what is the elementary excitation in this case. Resonant Raman scattering was found in this experiment. The core exciton and valence exciton will play important roles in the Raman-scattering effect.

II. EXPERIMENT

Soft-x-ray emission measurements were carried out by the SXES system[7] which is installed at the beam line BL-19B at Photon Factory, KEK. As the excitation light source, the Revolver Undulator[8] was used. A VLM19 monochromator[9] with a varied-line spacing plane grating whose average groove density is 2400 lines/mm was used. By using this beam line, a strong intensity light was achieved with a high-energy resolution. The calculation of the ray tracing shows that the resolution of the monochromator is obtained to be about 9 meV for the photon energy at 90 eV by using a 10-μm slit width. All the measurements of SXES and total SXE yield (TY) were measured by using 10-μm slit width of the VLM19 monochromator in this study. An optically polished (100) surface of Si crystal was used. The sample was cooled by a He cryostat. All the measurements were carried out at 18 K. The base pressure of the experimental system was about 2×10^{-11} torr.

In the SXES system,[7] a high-sensitivity position-sensitive detector and a 5-m concave grating with a groove density of 600 lines/mm were used. The detector was set at Rowland circle perpendicularly to the tangential plane of the Rowland circle. The overall resolution of the SXES was about 0.5 eV at the center of the detector, and about 0.8 eV toward the end of the detector. The typical signal count was about 30–50 counts per second (cps), with a background of about 4 cps. We observed the emitted SXE light at a large glancing angle, where the excitation light is incident on the sample at a very small glancing angle to avoid the self-absorption effect. The TY was measured by collecting all the SXE light. Since the detector of the SXES has no sensitivity for the visible light, the TY was measured for the SXE light above 4 eV.

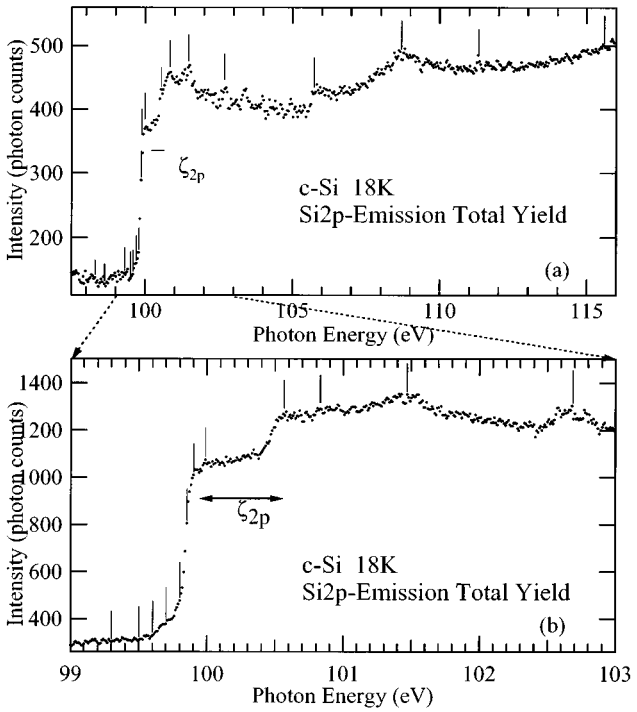

FIG. 1. Total yield of soft-x-ray emission spectrum of Si measured at 18 K. The vertical bars show the photon energies where the SXE spectra were measured. ζ_{2p} with an arrow shows the spin-orbit splitting of Si $2p$ core. The abscissa is the excitation photon energy. (b) in the lower panel shows the TY spectrum in the expanded energy scale of abscissa.

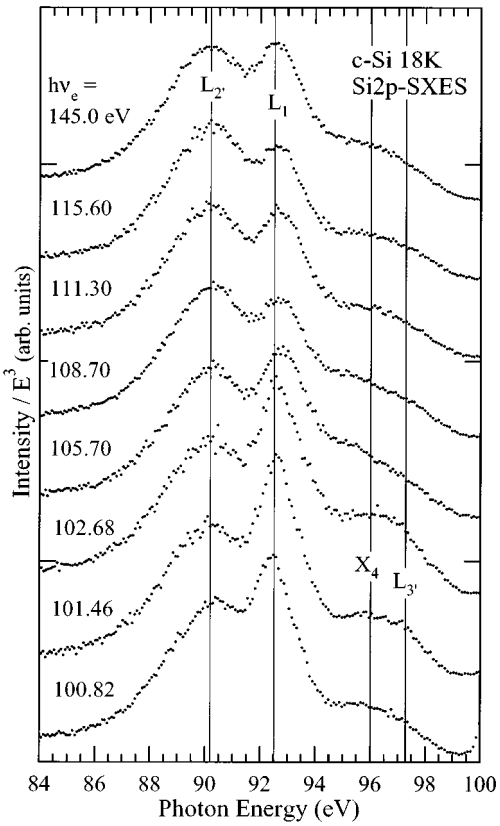

FIG. 2. The $L_{2,3}$ SXE spectra of Si measured at various photon energies that correspond to the excitation to the conduction bands. The abscissa is the SXE photon energy. The ordinate is the SXES intensity divided by the cube of the photon energy.

The calibrations of the VLM19 monochromatic and the SXES spectrometer are very important, because the SXE and TY spectra are plotted in the same abscissa in this study, which will give us important information about the total DOS for both the filled and empty states. The calibration of the VLM19 monochromator was carried out by the photoemission of the gold which was evaporated on the sample holder. The SXES spectrometer was calibrated by measuring the reflection light of gold on the sample holder. The photoemission and the SXE can be measured at the same time by using the same excitation light in this experimental system.[7]

III. RESULTS AND DISCUSSION

Figure 1(a) shows the TY spectrum of silicon. The abscissa represents the excitation photon energy ($h\nu_e$). The TY spectrum in expanded scale is shown in Fig. 1(b). The TY spectra in Fig. 1 are very similar to those reported by various authors.[10–15] However, the structures in Fig. 1 are much sharper. In particular, the $L_{2,3}$ edge structure in Fig. 1 is very sharp, and its width is about 100 meV. Bianconi *et al.*[11] measured both the surface- and bulk-sensitive electron yield spectra by utilizing the difference in the surface sensitivity depending on the kinetic energy of the electron. The bulk-sensitive spectra obtained by Bianconi *et al.* become sharp compared with the ordinary TY spectra. The total SXE yield spectra are, of course, much more bulk sensitive than any electron yield spectra. Thus, because of the lack of the surface-sensitive TY structure, as well as the low-temperature measurement, the SXE TY is much sharper than the electron TY. A doublet structure of 100.72 and 101.36 eV is clearly observed, and is attributed to the spin-orbit splitting (ζ_{2p}) of silicon. The bands at 102.7 and 103.3 eV are also spin-orbit splitting structures. The vertical bars in Figs. 1 indicate the photon energies at which the SXE spectra were measured. The doublet structure of 100.72 and 101.36 eV has been assigned to be L_1 conduction band, and that of 102.7 and 103.3 eV has been assigned to the L_4 conduction band.

The $L_{2,3}$ SXE spectra of silicon are shown by dots in Fig. 2, when the core hole is excited to the conduction band in higher photon energy region than the $h\nu_e = 100.82$ eV. The abscissa represents the SXE photon energy ($h\nu_{\mathrm{SXE}}$). The ordinate is the SXE intensity divided by E^3 in order to compare with the DOS curve.[16] Spectral features of SXE spectra are very similar to those of the spectra which were already measured by several authors.[5,6,17–20] These structures have been well elucidated by the total DOS. The two strong structures at around $h\nu_{\mathrm{SXE}} = 90.2$ and 92.5 eV have been assigned to the high DOS around $L_{2'}$; and L_1 bands. The L_1 SXES band located at lower-energy side becomes stronger for the lower excitation energy. The broad and weaker structures around $h\nu_{\mathrm{SXE}} = 96.0$ and 97.3 eV have been assigned to be X_4 and $L_{3'}$ valence bands.

Figure 3 shows both the SXE spectrum measured at $h\nu_e = 145.0$ eV (closed circles) and the TY spectrum (open circles), in order to compare with the total DOS (solid line).[21] It has been known that the structures of Si in the total

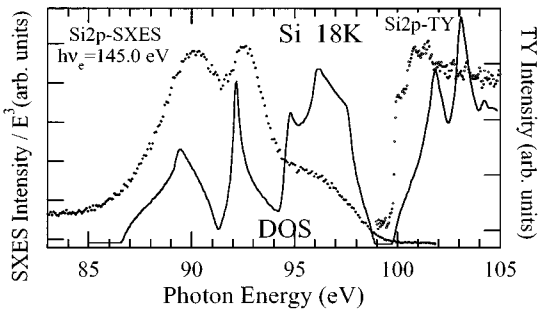

FIG. 3. The SXE spectrum of silicon measured at $h\nu_e = 145.0$ eV, and the TY spectrum in comparison with the total DOS curve (Ref. 21).

DOS are due to the high density of states which come mainly from L high-symmetry points, and the SXE spectrum seems to be consistent with the band calculation. The intensity of the calculated total DOS at $h\nu_{\mathrm{SXE}} = 95 \sim 100$ eV is much stronger, and its intensity at $h\nu_{\mathrm{SXE}} = 85 \sim 95$ eV is weaker than that of the experimental SXE spectrum. It is well known that the $3s$ components are dominant in the valence band at higher binding (lower photon) energy, while the $3p$ components are strong at the lower binding (higher photon) energy. Since the $L_{2,3}$ SXES reflects s and d partial components in the DOS, the $L_{2,3}$ SXES of silicon shows the different intensity ratio from the structures in the total DOS. On the other hand, it is known that the photoelectron spectra show a similar intensity ratio to the structures in the DOS spectra.

The SXES study has the characteristic merit that the SXE and TY can be plotted on the same abscissa (that is, photon energy), so that they are easily compared with the band calculation of both the valence and conduction bands. In fact, there is a remarkable difference between the TY spectrum and the conduction-band minimum of the DOS in Fig. 3. The TY spectrum has a sharp edge. The intensity of the TY is much stronger, and shifts slightly to lower energy. This difference has been already discussed, and has been assigned to be a core-exciton structure at the Δ-X line around the X_1 conduction band.[10–14,22,23] The quantity of the energy shift is not clear, though there is some shift. This shift corresponds to the binding energy of the core exciton.

Rubensson *et al.*[5] measured the excitation-photon-energy dependence of Si $L_{2,3}$ SXE spectra. The intensity ratio of the two main L_1 and $L_{2'}$ bands varies in accord with the $L_{2,3}$ absorption spectra. Furthermore, Miyano *et al.*[6] found that the X_4 band becomes strong when the core hole is excited to the state at the $L_{2,3}$ absorption edge. On the other hand, excitation-photon-energy dependence is not found in amorphous Si. Thus the excitation-photon-energy dependence is due to the **k** conservation rule of the core hole and the excited electron in the Si crystal.

Figure 4 shows the photon-energy dependence of SXES in the energy region of the core-exciton state which is formed near the $L_{2,3}$ absorption edge. The intensity ratio of two L_1 and $L_{2'}$ bands becomes reversed at $h\nu_e = 99.99$ eV. At the excitation energy below $h\nu_e = 98.50$ eV, which is located at just the $L_{2,3}$ absorption edge, it is found that a structure at $h\nu_{\mathrm{SXE}} = 91.1$ eV in SXES increases instead of both L_1 and $L_{2'}$ bands. To our knowledge, this band has not been found before now. Furthermore, the X_4 structure at

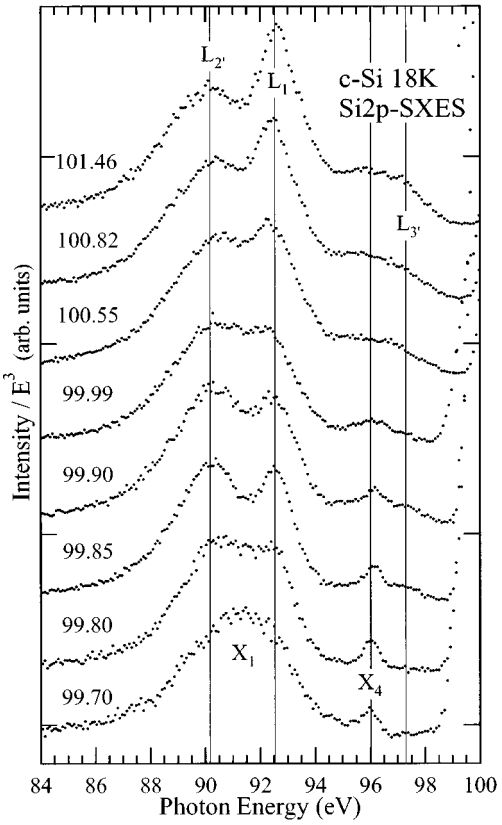

FIG. 4. The $L_{2,3}$ SXE spectra of Si measured at various photon energies in the $L_{2,3}$ core-exciton-energy region. The abscissa is the SXE photon energy. The ordinate is the SXES intensity divided by the cube of the photon energy.

$h\nu_{\mathrm{SXE}} = 96.0$ eV becomes clear, while the $L_{3'}$ band becomes weak and finally disappears.

In order to know the origin of the band at $h\nu_{\mathrm{SXE}} = 91.1$ eV, we compare the SXE spectra with the band dispersion curve. Figure 5 shows Si $L_{2,3}$ SXE spectra measured at $h\nu_e = 101.46$ and 99.70 eV and the TY spectrum, as well as the band dispersion curve which was calculated by Chelikowsky and Cohen.[21] The band dispersion curve is adjusted to the SXE spectra to coincide with the valence-band maximum. Three $L_{2'}$, L_1, and $L_{3'}$ valence bands are found at $h\nu_{\mathrm{SXE}} = 90.2$, 92.5, and 97.3 eV, respectively, in the SXE spectrum measured at $h\nu_e = 101.46$ eV. On the other hand, two X_1 and X_4 valence bands are found at $h\nu_{\mathrm{SXE}} = 91.1$ and 96.0 eV in the SXE spectrum measured at $h\nu_e = 99.70$ eV. Thus the band at $h\nu_{\mathrm{SXE}} = 91.1$ eV is found to be the X_1 valence band. Furthermore, the spin-orbit splitting at 100.72 and 101.36 eV in the TY spectrum is assigned to be an L_1 conduction band. The spin-orbit splitting at 102.7 and 103.3 eV is assigned to be an L_3 conduction band. Of course, the conduction minimum is assigned to be around the X_1 band along the X-Δ line. The coincidences of the SXES structures with the X bands are rather good within $0.1 \sim 0.2$ eV, while those with the L bands are not so good. The total bandwidth of the calculated band dispersion of the L bands is wider by about 1 eV than the experimental results obtained by both the SXE and TY spectra. Angle-resolved photoemission spectra of Si have been measured, but the structures at high binding energies, such as L_1, X_1, and $L_{2'}$ valence bands,

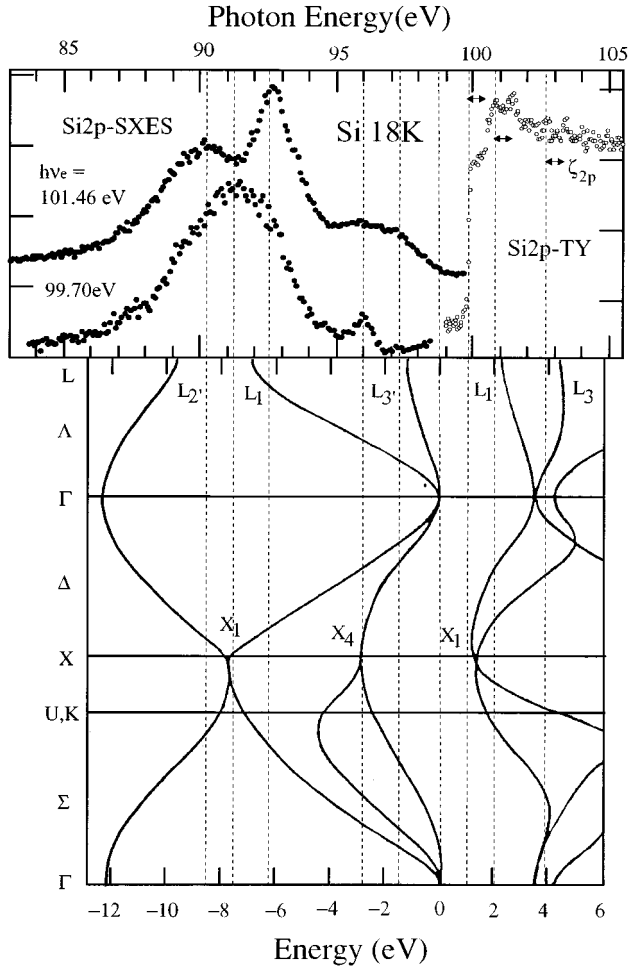

FIG. 5. The SXE spectrum of silicon measured at $h\nu_e = 101.46$ and 99.70 eV, and the TY spectrum in comparison with the band dispersion curve (Ref. 21).

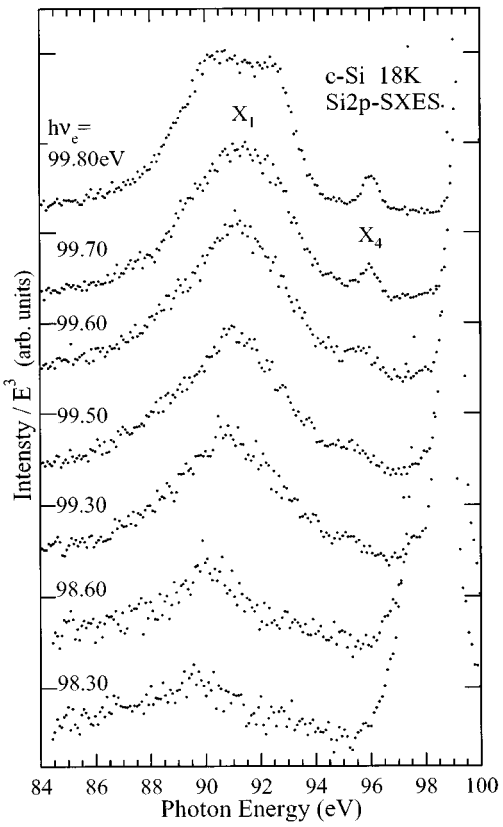

FIG. 6. The $L_{2,3}$ SXE spectra of Si measured at various photon energies that correspond to the excitation to the virtual states below the $L_{2,3}$ core exciton. The abscissa is the SXE photon energy. The ordinate is the SXES intensity divided by the cube of the photon energy.

are not so clear.[24,25] Therefore, it is difficult to compare our SXES results with the angle-resolved PES results.

It is found that the intensity of X_1 and X_4 valence bands becomes strong when the core electron is excited to the X_1 conduction-band minimum. When it is excited to the other bands where the L density is dominant, the intensity of the L_1 and $L_{2'}$ valence bands becomes strong. The **k** conservation model in the SXES process also seems to be consistent with our experiments. Thus the X_1 band is found only by excitation at the X_1 conduction-band minimum.

Figure 6 shows the SXE spectra that are measured in the photon-energy region below the $L_{2,3}$ threshold. As shown by the closed circle in Fig. 8, the SXES intensity drastically decreases with the decreasing photon energy. However, the SXES can be found at any excitation photon energy, irrespective of the lower excitation energy below the $L_{2,3}$ edge. These spectra are nothing but the Raman-scattering spectra that excite to the virtual state lower than the real state. It is clear that the main X_1 SXES band around $h\nu_{\mathrm{SXE}} = 91.1$ eV shifts to lower energy in proportion to the excitation photon energy. The line shape of this X_1 band seems to be the same, but becomes weak as the photon energy becomes low. Conversely, the small X_4 structure at $h\nu_{\mathrm{SXE}} = 96.0$ eV also shifts to lower energy, but the line shape becomes broad and weak in accord with the excitation energy.

Figure 7 shows the same figures as those in Fig. 6, where the abscissa is the Raman shift that is the energy shift from the excitation photon energy. In Fig. 7, it is clear that the X_1 and X_4 bands have the same Raman shift energy. The X_1 band has a Raman shift energy of 8.6 eV, and the X_4 band has a Raman shift energy of 3.9 eV. Since the energy shift does not change by the excitation photon energy, it is found that all these structures are not in the fluorescence band but the Raman-scattering band. The open circles represent the SXE spectrum measured at $h\nu_e = 98.30$ eV that is factored by 50. The spectrum at 0 eV corresponds to the Rayleigh scattering peak. It is found that the intensity ratio of the Raman scattering and the Rayleigh scattering is about 150 in the SXE spectrum measured at $h\nu_e = 98.30$ eV.

Figure 8 shows the photon-energy dependence of the intensity of the Raman (closed circles) and the Rayleigh scattering (open circles). These spectra are obtained so that the sum of both intensities becomes the TY spectrum. The intensity of the Raman scattering is almost zero at lower photon energy, as opposed to the $L_{2,3}$ edge, and has no background intensity. It increases gradually toward a photon energy of 99.60 eV and then drastically increases to 99.90 eV. This change of the intensity clearly shows the resonant Raman effect, and the resonant state is the X_1 core-exciton state at the $L_{2,3}$ edge. It is well known that the resonant Raman-scattering intensity should increase rapidly by the Kramers-

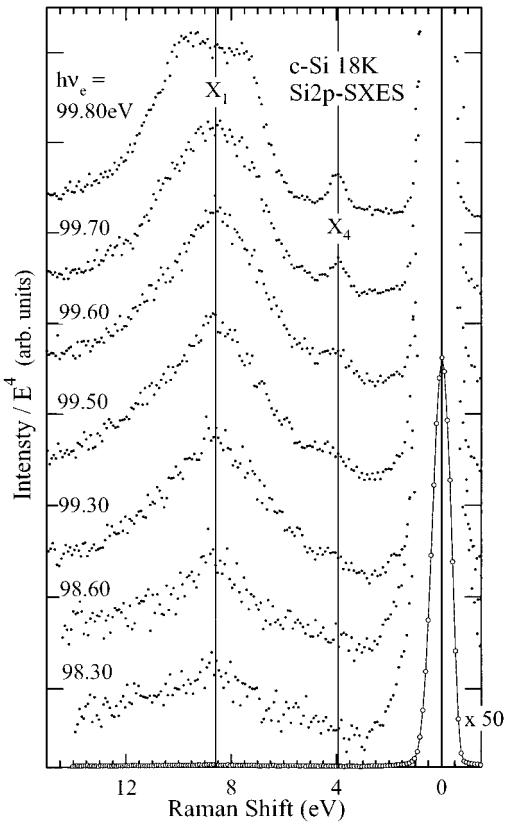

FIG. 7. The Raman spectra of Si in the energy region below the $L_{2,3}$ core exciton. The ordinate is the Raman intensity divided by E^4. The abscissa is the Raman shift energy that is the energy shift from the excitation photon energy.

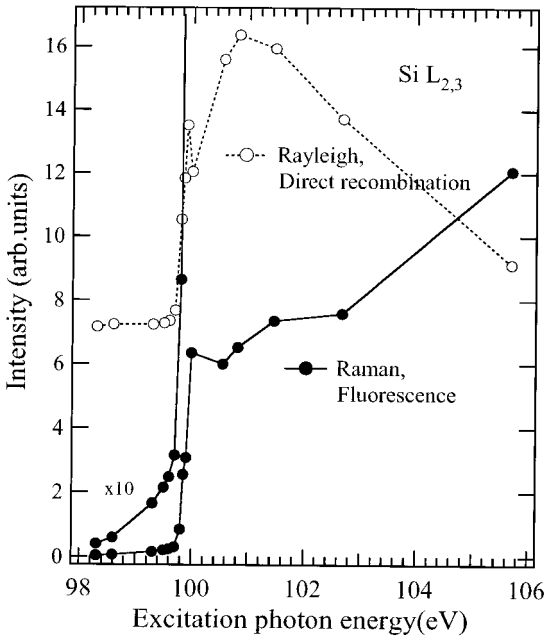

FIG. 8. Open circles show the intensity of the Rayleigh scattering and the direct recombination light. Closed circles show the intensity of the Raman and fluorescence light.

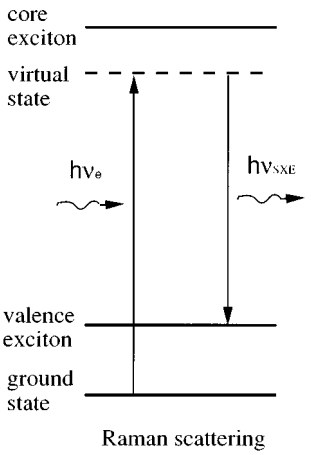

FIG. 9. Schematic energy diagram of the Raman scattering process at the Si $L_{2,3}$ exciton region. The elementary excitation of the Raman scattering is the X-point valence-band excitons. The intermediate state of the ordinary Raman process is the virtual state. The ordinary Raman process converges to the resonant Raman process continuously, as the photon energy comes close to the core-exciton state.

Heisenberg formula. Conversely, the intensity of the Rayleigh scattering is similar to the TY spectrum, and it has a constant background intensity below the $L_{2,3}$ edge. The Rayleigh-scattering intensity decreases and comes close to the background intensity, as the excitation photon energy increases far above the $L_{2,3}$ absorption edge. On the other hand, the SXES intensity becomes stronger. This fact shows that the intensity of the fluorescence band becomes stronger as the excitation photon energy increases far above the $L_{2,3}$ absorption edge.

On the other hand, the line shape of the Raman scattering seems to be similar below $h\nu_e = 99.70$ eV. The SXE spectra begin to change at a photon energy above $h\nu_e = 99.70$ eV. Thus it is found that the resonance effect takes place at the core-exciton structure which is formed at the X_1 conduction minimum. If these spectra are the Raman spectra, what is the elementary excitation in the Raman process? These Raman bands have 8.6- and 3.9-eV Raman-shift energies at the X_1 and X_4 bands, respectively. The final state after the Raman scattering is an electron at the X_1 conduction-band minimum that forms a core exciton state and a valence hole at X_1 or X_4 point. This final state is attributed to the transition from the valence band to the conduction band between two X points. Of course, it forms a valence exciton state at the X points. Since the electron at the X_1 conduction-band minimum changes from the core-exciton state to the valence-exciton state, the binding energies of the core and valence excitons become different. However, this difference cannot be found because of the small energy difference.

Figure 9 shows the schematic energy diagram of the Raman scattering on Si. For resonant Raman scattering, it resonates to the core-exciton state and emits a valence-band exciton as an elementary excitation of the Raman scattering. On the other hand, the intermediate state of the ordinary Raman-scattering process is the virtual state below the real X_1 core-exciton state in the resonant Raman scattering. Even in the case of ordinary Raman scattering, the elementary ex-

citation is also the valence-band exciton. The ordinary Raman process converges to the resonant Raman process continuously, as the photon energy comes close to the core-exciton state.

It is interesting that the valence-band exciton becomes broad and weak, as the resonant Raman process goes to the ordinary Raman process. In particular, broadening of the valence-band exciton located at 3.9 eV of the Raman shift which corresponds to the exciton from the X_4 valence band to the X_1 conduction band is evident. This band finally disappears at the normal Raman scattering. Here one should remember that the selection rule of the normal Raman scattering has been studied for a long time by ordinary laser Raman scattering. In this sense, the transition from X_1 to X_1 symmetry is a totally symmetric transition, so that the X_1 band is Raman active. Thus the line shape of the X_1 band does not change drastically. On the other hand, the transition from the X_4 valence band to the X_1 conduction band is a dipole-allowed transition, and is not Raman active when we consider the group theory. It is known that the dipole transition and Raman bands have complementary selection rules[26] for the ordinary Raman process, when the crystal structure has a centrosymmetry. Thus it is reasonable that the X_4 band is not observed in normal Raman-scattering process. Furthermore, it is also known that the Raman selection rule often breaks at the resonant Raman process. Therefore, the dipole-active X_4 band might have some intensity at the resonance state because of the breakdown of the selection rule at the resonant state. Of course, the microscopic mechanism of the excitation energy dependence of these Raman bands has not been studied at all. A theoretical study will be needed to solve it. In particular, the phonon effect may play an important effect in the excited state. In this study, one finds even in the soft-x-ray region that there is the microscopic problem of the resonant Raman scattering that used to be found in laser Raman scattering.

If we put the resonant Raman-scattering process at the Si $L_{2,3}$ absorption edge into other words, as in Fig. 9, the core-exciton state in the intermediate state is exchanged with the valence-band exciton in the final state. This fact shows that there is an interaction between the core exciton and the valence exciton, and that it plays an important role in the Raman-scattering process. Although the detailed mechanism is not known, this effect will raise another problem in soft-x-ray emission studies.

IV. CONCLUSION

A SXES study at the Si $L_{2,3}$ absorption edge has been carried out by using synchrotron radiation with a very high-resolution energy as an excitation light. The resonant Raman process has been found at an X_1 core exciton. Normal Raman scattering has also been found, and its intensity grows drastically as the excitation energy comes close to the resonant state. As an elementary excitation, the valence-band exciton that is formed from the X_1 or X_4 valence states to the X_1 conduction-band minimum is emitted in the Raman process. The X_4 valence exciton has a characteristic excitation-energy dependence, so that it becomes broad and weak as the resonant Raman process goes to the ordinary Raman process.

ACKNOWLEDGMENTS

We would like to thank Professor K. Nasu for his helpful discussions. We also are grateful to the staff of the Photon Factory, KEK for their excellent support.

[1] J. Nordgren, in *New Directions in Research with Third-Generation Soft X-Ray Synchrotron Radiation Sources*, edited by A. S. Schlachter and F. J. Wuilleumier (Kluwer, Dordrecht, 1994), p. 189; D. L. Edreer, K. E. Miyano, W. L. O'Brien, T. A. Callcott, Q.-Y. Dong, J. J. Jia, D. R. Mueller, J.-E. Rubensson, R. C. C. Perera, and R. Shuker, *ibid.*, p. 281.

[2] Y. Ma. N. Wassdahl, P. Skytt, J. Guo, J. Nordgren, P. D. Hohnson, J.-E. Rubensson, T. Boske, W. Eberhardt, and S. D. Kevan, Phys. Rev. Lett. **69**, 2598 (1992).

[3] P. D. Johnson and Y. Ma, Phys. Rev. B **49**, 5024 (1994).

[4] P. Skytt, P. Glans, D. C. Mancini, J.-H. Guo, N. Wassdahl, J. Nordgren, and Y. Ma, Phys. Rev. B **50**, 10 475 (1994).

[5] J.-E Rubensson, D. Mueller, R. Shuker, D. L. Ederer, C. H. Zhang, J. Jia, and T. A. Callcott, Phys. Rev. Lett. **64**, 1047 (1990).

[6] K. E. Miyano, D. L. Ederer, T. A. Callcott, W. L. O'Brien, J. J. Jis, L. Zhou, Q.-Y. Dong, Y. Ma, J. C. Woicik, and D. R. Mueller, Phys. Rev. B **48**, 1918 (1993).

[7] S. Shin, A. Agui, M. Fujisawa, Y. Tezuka, T. Ishii, and N. Hirai, Rev. Sci. Instrum. **66**, 1584 (1995).

[8] G. Isoyama, S. Yamamoto, T. Shioya, J. Ohkuma, S. Sasaki, T. Mitsuhashi, T. Yamakawa, and H. Kitamura, Rev. Sci. Instrum. **60**, 1863 (1989).

[9] M. Fujisawa, A. Harasawa, A. Agui, M. watanabe, A. Kakizaki, S. Shin, T. Ishii, T. Kita, T. Harada, Y. Saitoh, and S. Suga, Rev. Sci. Instrum. **67**, 345 (1996).

[10] F. C. Brown, R. Z. Bachrach, and M. Skibowski, Phys. Rev. B **15**, 4781 (1977).

[11] A. Bianconi, R. Del Sole, A. Selloni, P. Chiaradia, M. Fanfoni, and I. Davoli, Solid State Commun. **64**, 1313 (1987).

[12] X. Weng, P. Rez, and P. E. Batson, Solid State Commun. **74**, 1013 (1990).

[13] P. E. Batson, Phys. Rev. B **44**, 5556 (1991).

[14] P. E. Batson, Phys. Rev. B **47**, 6898 (1993).

[15] *Synchrotron Radiation Research, Advances in Surface and Interface Science*, edited by R. Z. Bachrach (Plenum, New York, 1992).

[16] D. H. Tomboulian, *X-Rays* (Springer-Verlag, Berlin, 1957).

[17] P. Livins and S. E. Schnatterly, Phys. Rev. B **37**, 6731 (1988).

[18] P. A. Bruhwiler and S. E. Schnatterly, Phys. Rev. B **39**, 12 649 (1989).

[19] M. Iwami, H. Nakamura, M. Hirai, M. Kusaka, Y. Azuma, and F. Akao, Jpn. J. Appl. Phys. **29**, L470 (1990).

[20] M. Iwami, M. Hirai, M. Kusaka, M. Kubota, S. Yamamoto, H. Nakamura, H. Watabe, M. Kawai, and H. Soezima, Jpn. J. Appl. Phys. **29**, 1353 (1990).

[21] J. R. Chelikowsky and M. L. Cohen, Phys. Rev. B **14**, 556 (1976).
[22] M. Altarelli and D. L. Dexter, Phys. Rev. Lett. **29**, 1100 (1972).
[23] F. Evangelisti, F. Patella, R. A. Riedel, G. Margaritondo, and P. Fiorini, Phys. Rev. Lett. **53**, 2504 (1984).
[24] A. L. Wachs, T. Miller, T. C. Hsieh, A. P. Shapiron, and T.-C. Chiang. Phys. Rev. B **32**, 2326 (1985).
[25] D. H. Rich, G. E. Franklin, F. M. Leibsle, T. Miller, and T.-C. Chiang. Phys. Rev. B **40**, 11 804 (1989).
[26] S. Shin, Y. Tezuka, A. Sugawara, and M. Ishigame, Phys. Rev. B **44**, 11 724 (1991).